Contents lists available at ScienceDirect



Separation and Purification Technology

journal homepage: www.elsevier.com/locate/seppur



Membrane aging effects on water recovery during full-scale potable reuse: Mathematical optimization of backwashing frequency for constant-flux microfiltration

N.G. Cogan a,*, Deniz Ozturk a, Kenneth Ishida b, Jana Safarik b, Shankararaman Chellam c

- ^a Department of Mathematics, Florida State University, 208 Love Building, Tallahassee, Fl 32306, United States of America
- b Principal Scientist, Orange County Water District, 18700 Ward Street, Fountain Valley, CA 92708, United States of America
- Departments of Civil and Environmental Engineering and Chemical Engineering, Texas A&M University, College Station, TX 77843, United States of America

ARTICLE INFO

Keywords: Potable reuse Mathematical modeling Optimal control Hollow fiber Fouling control Wastewater reclamation

ABSTRACT

One tool in efforts to tackle the ever growing problem of water scarcity is municipal wastewater reclamation to produce drinking water. Microfiltration (MF) is a central technology for potable reuse because it is highly effective in removing pathogenic protozoa, bacteria, and other colloids and for reverse osmosis pretreatment. However, as microfiltered materials accumulate at the membrane surface, its productivity is reduced requiring periodic removal of foulants. A mathematical model of MF is described in the context of hollow fiber filtration that focused on optimizing constant flux operation with backwashing. Design curves were also proposed for determining backwash timing. The model analysis is evaluated against real-world MF fouling for membranes that range in age from a few weeks to three years, observed at the world's largest water reuse facility operated by the Orange County Water District. The presented model compares well with the full-scale operational data, and model parameters accurately capture variations in fouling kinetics with membrane age, providing clues to changes in optimal regeneration timing and frequency as membrane performance declines over long time scales.

1. Introduction

The global water scarcity has been well-documented, with approximately 4 billion people experiencing severe shortage at least one month annually and over 500 million experiencing it throughout the year [1]. This problem is only predicted to worsen with 700 million people facing displacement due to intense water scarcity in the next decade [2]. Given that a third of the world's largest groundwater basins are distressed [3] and excessive groundwater utilization causes ground subsidence that worsens flooding and damages the built infrastructure [4], a logical approach to tackle water scarcity is to better utilize surface water sources and to implement potable water reuse.

It is imperative to treat impaired waters to ensure public health and safety before they can be distributed to the serving public, with municipal wastewater reuse demanding much more extensive treatment. Microfiltration (MF) and ultrafiltration (UF) effectively separate particulate contaminants including turbidity and pathogenic microorganisms such as protozoa and bacteria from contaminated water sources [5]. MF and UF share numerous characteristics (except for nominal pore size), typically discussed together as "low-pressure membrane processes", and are both oft-employed for surface water treatment and

as a pretreatment to reverse osmosis or nanofiltration in potable reuse applications [5,6]. MF/UF are also commonly used in bioseparations, food and beverage processing, and other industrial applications [7–10]. Unsurprisingly, in all cases, removed materials accumulate at or near the membrane surface and inside the pores reducing productivity and hindering their wider implementation. In the case of Orange County Water District (OCWD), MF was chosen for RO pretreatment and thus this article focuses on MF fouling.

Periodic removal of the foulants is key to efficient membrane operation [6,11]. Maintaining tangential shear to scour away foulants is one fouling control method [8,12,13], which in some extreme cases does not effectively maintain productivity [14,15]. In contrast, deadend operation with periodic backwashing dominates municipal water/wastewater treatment and water reuse applications because it is capable of maintaining productivity and a high water recovery [6,16]. Backwashing interrupts forward filtration and uses MF permeate during flow reversal to dislodge accumulated foulants. Hence, backwashing too often will reduce water recovery while maintaining MF productivity, whereas reducing backwashing frequency can be expected to

^{*} Corresponding author.

E-mail address: cogan@math.fsu.edu (N.G. Cogan).

lower membrane permeability while increasing recovery indicating a potential optimal mode of backwashing and recovery.

Outside-in, hollow fiber geometry provides a high packing density while simultaneously facilitating backwashing and chemical cleaning; therefore, it is currently the preferred geometry in nearly all microfilters employed for long-term environmental and industrial applications [17,18]. To date, optimization of backwash timing for hollow fiber membranes has largely focused on empirical investigations e.g. [6, 19-21]. Importantly, the fluid mechanics depends strongly on membrane geometry, apparently disallowing direct extension of results from one geometry to the other [22-24]; however, mathematically rigorous and tractable models that neglect the geometrical details can still be used to understand the role of membrane age and other characteristics in the context of backwash timing and MF operation. Relatively simple, mathematically tractable models have been shown to be able to capture the relevant filtration information e.g. [25]. To develop any analytic method, optimal control approaches typically require simplified models [26,27]. This framework has been developed to address MF in increasingly complex situations, from weakly interacting and easily removable foulants, to biologically active foulants that cause irreversible fouling, etc. [26,28]. The current study is aimed at three extensions that provide useful insights into MF as well as the flexibility of the model structure. First, the model is formulated in constant flux operation by focusing on the increasing pressure required to obtain a constant flux of fluid as the filter fouls dynamically. The second task is to consider whether this class of spatially homogeneous models can be used to address other geometries. The applicability of this model to the performance of hollow fiber microfilters from the world's largest water reuse facility at the OCWD Advanced Water Purification Facility (AWPF) is then evaluated. In other words, it is determined whether neglecting the microfilter geometry (specifically, models that do not depend explicitly on spatial dimensions) has a profound effect on model parameters and fouling predictions by comparing an ordinary differential equation model that neglects spatial geometry to data obtained from hollow fiber filters. In previous studies, results were compared directly with data obtained from flat-sheet filtration where a spatially homogeneous model is a less stringent assumption. A model that neglects details including treatment of the multidimensional fluid dynamics, detailed modeling of the physical mechanisms of pore fouling are not needed to capture the dominant time scales and dynamics of the fouling and regeneration process. This is very important since along with the goals of demonstrating that the current spatially homogeneous model can be parameterized using full-scale data, it is of interest to determine how the membrane aging alters the predictions in terms of optimal reversal timing and frequency which is substantially more complicated and uncertain for more complicated models.

Finally, analyzing the model from the perspective of optimal control provides a way to relate optimization to membrane age by pursuing deteriorations in water productivity over a long timeframe. Multiple days of observations, spaced by several months are used to provide average behavior over three years. Polymeric membranes are known to lose productivity over long time-scales due to hydraulically and chemically irreversible fouling coupled to polymer degradation associated with attack by disinfectants used for chemical cleaning and/or biofilm control during regular operation [29–32].

Prolonged exposure to strongly interacting foulants and harsh oxidants, typically over a few years, has been documented to change membrane morphology and surface chemistry thereby negatively impacting performance e.g. [33,34]. Given the inherent complexities in modeling large-scale membrane plants, only empirical data are available to date on aging of low-pressure membranes [33]. Hence, relating membrane age even qualitatively to model parameters constitutes a useful contribution to membrane operation and design engineers.

The main goal of this manuscript is the mathematically rigorous optimization of backwashing time courses and durations to minimize the pressure increases and maximize productivity, i.e. permeability.

A closely related and important technological aspect of the work is implementing the model to assess differences in parameters as the filter ages. The variation in parameter estimates over time are then determined. This leads to insights into the aging processes as well as indications for how to adjust the cleaning regime as the membrane ages. In the next section, our recent model of constant pressure MF with backwashing [26] is reviewed and reformulated in terms of the permeability for constant flux mode. A discussion of the parameterization of the model using data provided by the OCWD for two MF cells from their AWPF follows. Finally, the optimal control methodology is described and insights gained from the model analysis and how this method connects with practical implementation are discussed.

2. Model development

Microfiltration operation occurs in multiple steps. First, during the forward operation, the contaminated water is forced or drawn through the membrane. During forward operation, foulants accumulate on the surface, which hinders the transport of water across the membrane. Following the development in earlier publications [26,28], the accumulation of foulant, B, on the surface of a membrane during forward filtration is assumed to be proportional to the flux, J, across the membrane. We further assume full retention of the foulant.

A portion of the foulants deposited during forward filtration is removed from the filter by reversing the flow. In real-world systems, when the pressure required to achieve the target flux reaches operational constraint (1 psi or 6894.76 Pa in the case of OCWD), the flow is reversed by reversing the pressure drop. The flow reversal is referred to as backwashing or regeneration and is a technique often employed for MF regeneration. During regeneration, the foulant is assumed to be removed at a rate proportional to the product of the flux and the amount of foulant that has accumulated on the membrane. This rate may depend on other aspects of the operation, for example, irreversible fouling [28], where the rate of removal decreases depending on the timing of the forward operation through the formation of a difficult to detach layer, e.g. biofilm.

The complexity of the system depends on the application/experiments that provide the data to parameterize the model. Similarly, there may be a pause between forward operation and regeneration. The membrane may be further treated using air scouring, or chemical treatment to overcome irreversible attachment and long-term fouling. Here, OCWD specifically backwashes frequently in an effort to minimize irreversible fouling. Irreversible attachment, air-scouring and short pauses between forward operation and regeneration will be neglected hereafter. This simplifies the model and allows us to analyze the optimal control problem directly, although this may restrict the validity of long-term analysis. It is not at all abnormal to close a model and include some quantities that vary (e.g. water quality) in parameters. Especially given the lack of first principles hypotheses for which to derive a model for the evolution of water quality (see Table 1).

Forward operation and regeneration are distinguished using a piecewise constant function, u(t) that takes the value 1 during forward filtration and -1 during regeneration. The equation governing the dynamics of the density of foulant on the surface of the membrane, B.

$$\frac{dB}{dt} = \frac{(1+u)}{2}KJ - \frac{(1-u)}{2}\hat{K}JB,$$
(1)

where K and \hat{K} describe the foulant accumulation and removal, respectively. This is the model developed in [26,28]. Note that when u=1, the right-hand-side of Eq. (1) becomes the constant rate KJ indicating an increase in foulant proportional to the flux through the filter. When u=-1, the right-hand-side becomes $-\hat{K}JB$ indicating a decrease in accumulated foulant at a rate proportional to the flux. This neglects some details of the fouling including irreversible fouling since \hat{K} varies over the time-scale of membrane aging and not on the time-scale of

fouling and regeneration (e.g. \hat{K} is held constant over the duration of each panel in Fig. 1). In contrast to previous studies [26,28], the focus here is on constant flux operation but still considering iterating between forward and backwards operation. In this notation, the flux is the same; however, the different scaling parameters, K and \hat{K} , could be interpreted as different flux values for filtration or regeneration.

There is feedback between foulant accumulation and the flux that describes the effect of fouling on the filter operation since the dominant source of fouling considered is due to material accumulation on or near the membrane. It is typical to use a resistance in series relationship between the pressure and flux when modeling MF,

$$J = \frac{\Delta P}{(R_m + R_R)},\tag{2}$$

where R_m denotes the fixed membrane resistance which is the product of the absolute viscosity and the typical membrane resistance and R_B which is resistance that increases as the foulant accumulates. The coupling between the foulant and the flux/pressure is through $R_B = \gamma_b B$ where γ_b is interpreted as the product of the absolute viscosity and resistance due to membrane foulant. This model has been used in several previous studies and has been shown to accurately capture data from multiple sources [26,28,35,36]. Additionally, although the details of the formulation allow for analytic solutions, the general framework described here is quite generic. Given the variety of data fits that are demonstrated, it appears that these assumptions are not overly restrictive.

Since J is constant, the differential equation in Eq. (1) is solved analytically by separating forward and backwards operation. The details are given in the Appendix. Accumulation during cycles of forward and backwards operations is obtained by composing the solutions for each phase. Variables, parameters and units are given in $\ref{eq:solution}$?

3. Materials and methods

During the time of the study (the years 2017-2020), the AWPF MF system was designed to produce 4.38 m³/s of filtrate as feed to the RO system at a designed flux of 34 L/m²/h. It consisted of 36 Memcor CS Evoqua Continuous Submerged MF system cells [37]. The Memcor CS system is an induced flow process where water is drawn through the membrane module using the pressure differential (pressure between the feed side and filtrate side of the membrane module) developed from the suction side of the filtrate pump. The modules are submerged in a process feedwater tank, which is open to the atmosphere. Each cell holds up to 684 polypropylene hollow fiber membrane modules with a nominal pore size of 0.2 µm and operates at a water recovery rate between 88% and 90%. Per the operational requirements of OCWD, every 22 min the membranes are backwashed (to remove solids buildup by a combination of air scouring the surface of the fibers, reverse liquid flow from the inside to the outside of the fibers and draining the membrane tank to remove the solids). The Memcor CS system treats secondary effluent that receives up stream chloramination of 3-5 mg/L through addition of 12.5% sodium hypochlorite. The feedwater contains sufficient ammonia (2.5 mg/L as NH3-N) to form chloramines when hypochlorite is added. Only trace amounts of ammonia remain and the chloramine (disinfectant) residual remains through the entire MF, RO, and ultraviolet — advanced oxidation process (UV-AOP). The MF system produces a low turbidity product water with a silt density index (SDI) below 3 necessary for successful RO operation downstream. Operational data from a unit over the course of three years of observation is considered for modeling purposes. The dataset comes from repeated observations of each unit. Rather than observe an arbitrary set of cycles, daily snapshots of observations (i.e. flow and transmembrane pressure measured every 5 s) at the same timeframe for each week are used. By treating each snapshot as an observation, means and standard deviations for the data are established. Note that this process leads to approximately 10,000 data points for each membrane

Table 1

Average MF feed and permeate water quality during the course of this study with standard deviations.

Characteristics	MF feed		MF effluent	
	Ave.	Std. dev.	Ave.	Std. dev.
Electrical Conductivity (μmho/cm)	1670	94.7	1680	100
Total Dissolved Solids (m g/L)	987	63.7	1010	51.5
Turbidity (NTU)	1.6	0.60	0.11	0.25
pН	7.3	0.1	7.1	0.1
Total Organic Carbon (m g/L)	9.6	1	7.8	0.5
Total coliform (MPN/100 ml)	32100	53900	<1	NA
Silica (m g/L)	20.6	2.6	20.9	2.8

age. Backwash cycles with flow and transmembrane pressure (ΔP) were measured every 5 s using real-time sensors.

Table 1 depicts important water quality parameters in the MF feed and permeate waters. The secondary-treated municipal wastewater was saline and contained relatively high concentrations of suspended solids, organic matter, bacteria, and silica. In other words, colloidal, organic, bacterial, and inorganic fouling would have simultaneously contributed to fouling necessitating an approach that combines all foulants into a single variable, *B*, as outlined in Section 2. Note that as expected, MF pretreatment successfully removed the vast majority of particulate matter (including turbidity, and coliform bacteria) and 25% of the total organic carbon consequently reducing fouling of downstream desalination membranes.

Note that physicochemical influent water quality parameters were relatively stable with coefficients of variation ranging between 1% (pH) and 19% (turbidity). In contrast, coliform bacteria varied significantly, as can be expected for microbiological parameters. These data suggest that changes in the influent water characteristics at the full-scale facility over the course of the 3-year span of monitoring membrane productivity could have influenced the results in addition to membrane aging.

4. Parameter estimation

Microfiltration membranes age predominantly due to irreversible fouling and/or physicochemical alterations arising from repeated exposure to aggressive chemicals used for regeneration [29–31,33,34,38,39]. Hence, it is necessary to consider hydraulically and chemically irreversible fouling in aging. In the model, foulant removal is described by the parameter \hat{K} that provides a measure of backwashing efficiency. Changes to the membrane morphology arising from exposure to strong chemicals and foulant accumulation are captured by the parameter R_m . The parameter γ_b captures the efficiency of fouling induced by accumulated material (see Eq. (3)). For example, this parameter is high for smaller colloids that tend to form less permeable cakes or materials that accumulate within the pores and restrict water permeation to a greater extent compared with surface deposition.

Importantly, although these model parameters broadly capture relevant engineering phenomena and it is benchmarked with data from a full-scale plant, there are other confounding factors, including variations in feed water quality that impact the results. Currently, no causal relationships to parameter variations are posited; however, the model is able to characterize the interaction between fouling, backwashing and filtration.

There are four key parameters that need to be estimated. The foulant accumulation rate, $K (\mathrm{gm^2/L^2})$ that provides some measure of the feed water quality. Large K occurs for water with high concentrations of foulants (e.g. organic matter and turbidity). The foulant removal is described by $\hat{K} (\mathrm{m^2/L})$ that provides a measure of backwashing efficiency. The specific parameter that describes the resistance due to foulant accumulation (or the fouling efficiency) is denoted $\gamma_b (\mathrm{L/(gm)})$ and depends on the foulant (e.g. particle size distribution). In other studies, resistance due to the build-up of dense, irreversibly attached

foulant (e.g. cake resistance) was included [28]; however, as discussed above, data were collected from units operating in conditions designed to minimize the build-up of any irreversible aggregates. The membrane resistance, denoted R_m (1/m), is originally determined by the nominal pore size, tortuosity, and membrane thickness. However, over the course of long-term operation, irreversible fouling, exposure to cleaning chemicals, and other factors change R_m , which is also an adjustable parameter herein [39,40].

A common method to analyze fouling with changing flux and/or pressure is to normalize the flux by the pressure and interpret the specific flux, which is similar to permeability with omitting the water viscosity. Comparisons using this are given throughout the remainder of the manuscript, since this is well-accepted in the membrane community. The local permeability of the membrane provides a means of comparison between constant flux and constant pressure operation.

$$J_{sp} = \frac{J}{\Delta P} = \frac{1}{(R_m + \gamma_b B)}.$$
 (3)

The parameter set that minimizes the discrepancy between observations and the model can be estimated from the analytic solutions. Recall that our observations were taken over 10 backwashing cycles. Specifically the parameters that minimize the sum of squares error between the calculated specific flux, $J_{sp,model}$ and the observed specific flux, $J_{sp,data}$ are determined. There are many methods available to determine the parameters. Note that the goal of any parameterization is to identify parameter values that minimize the discrepancy between the model predictions and observations. With a perfect model and perfect data there would be no discrepancy — differences between model predictions and observations are due to errors in data collection, variations in processes that are not fully accounted for, and other sources of uncertainty. The method described in [41] is applied here. This is a differential evolutionary method similar to simulated annealing. The basic concept is to search over parameter space, seeking parameters that minimize the error. Genetic algorithms take multiple random starting positions, estimate the error and then combine the best parameter sets (mimicking a mutation), to generate new parameter sets. Note that estimates using Nelder-Mead methods in Matlab (via fminsearch) and simulated annealing were essentially the same parameter sets — with genetic algorithms being much faster. In Fig. 1, the best fit predictions for the behavior of membrane units in increasing age of operation — up to 3 years are shown. Note that at OCWD, MF membranes are replaced every 5-7 years [42]. Hence, we captured about half their useful life in this manuscript and determined observable changes within that time-frame. In this time period, we see a decline of 52% in specific flux. This parameterization is a crucial step. Once estimates for the parameters are established that describe the state of the filter, optimization can be estimated while understanding that the optimal control problem is tuned to the state of the filter. Note that these units were not operated with the goal of optimization. The ratio of forward to regeneration time is essentially the same for each of the units (22 min filtration followed by ~ 3 min backwashing). The optimal control analysis described below indicates that this ratio does not optimize the water production. The parameters obtained are shown in Fig. 2. Since the fitting uses a stochastic method, the 100 fits were obtained and standard deviations are also shown in Fig. 2. Uncertainty was reduced by considering multiple observations and repeated parameter estimates, providing quantified confidence intervals.

To further explore this, the values of the parameters as functions of time are compared in Fig. 2. Considering the variation in parameters by comparing to longitudinal data provides insight into how processes change over time just as they would show insight if operational conditions are changed. There is an increase in the estimate of R_m after month 18, which is of lower magnitude than the changes seen in the other parameters. Notably, there is a sharp change in γ_b and K after month 21. An increase in K and a decrease in \hat{K} is consistent with the hypothesis that maintaining constant flux is more

difficult as membranes age. This has often been attributed to exposure to disinfectants and other "aggressive" chemicals over an extended duration although this model merely reflects this behavior through the parameter estimates [10,18,30,33,34,38,43]. It is possible that the decrease in γ_h may be explained by mechanisms associated with the surface accumulation to compensate for the increased accumulation while maintaining constant flux. Some of the parameter variability could also be attributed to influent water quality fluctuations that are unavoidable in any full-scale facility. More rigorous interpretations of the model parameters and their relationships to water quality and membrane operation is beyond the scope of this manuscript as herein we are primarily interested in how variations in estimated parameters affects optimal control predictions. This is determined by comparing optimal regeneration cycling for different parameter values that are consistent with different membrane ages. Specifically, we note in the next section that the optimal solutions depend directly on the parameters of the model. These changes are attributed to dynamic changes in the membrane composition that occurs over time since the typical water quality is closely monitored.

The observation is that continued, long-term operation contributes to irreversible fouling that eventually critically affects the fibers. The model does not address the specific mechanisms but does introduce the effect of aging on the microfilter productivity. Based on the age-dependent parameterization, it appears that there are abrupt changes after around 21 months of operation. In this three-year period, the average specific flux declined by 52%.

Recall that one of the main goals was to explore optimization, not just diagnosis. Using the estimated parameters, the optimization is explored in the next section.

5. Optimal control analysis

One of the fundamental goals of this manuscript is to find the optimal timing and duration of backwashing. This problem is viewed through the lens of classical, geometric, optimal control where the optimization (in this case maximizing) of a Lagrangian is defined via Pontryagin's principle [44]. In general, this is an extension of optimization of a function subject to a constraint as taught in a standard calculus sequences. The constraint in this case is a system of differential equations, and the goal is to maximize the Lagrangian functional. The piecewise constant control function, u(t), which maximizes the volume of water filtered (defined in the Lagrangian), subject to the constraint imposed by the fouling process (defined by the model ODEs) remains to be determined.

There are a large number of methods used to approach optimal control [44,45] with different strengths. Since the control, u(t), is a piecewise function, the optimal control problem is often referred to as a 'bang–bang' control problem [26]. It has been shown in several previous manuscripts that this approach leads to tractable and physically meaningful predictions [26,35,46,47].

One difficulty arises because u is piecewise defined and enters the Lagrangian linearly. Both of these require some care when defining the optimal control problem. This is handled by analyzing the problem temporarily assuming that u is a continuous variable and can take any value in the interval [-1,1], then standard 'bang–bang' methods handle the linearity of the control in the Lagrangian. Namely, u must take on the maximum or minimum values except for a curve, referred to as the switching curve, in the state/adjoint space where the control value is not defined. As shown in the Appendix, this curve can be determined based on the geometric properties.

This switching curve is a geometric curve that establishes the mixed trajectory that optimizes the problem. It is relatively straightforward to determine the value of the control function, u^* , so that the solution remains on the switching curve. Beginning with a clean membrane and filtering the water, the trajectory either never crosses the switching curve (in which case the optimal solution is to continuously filter) or

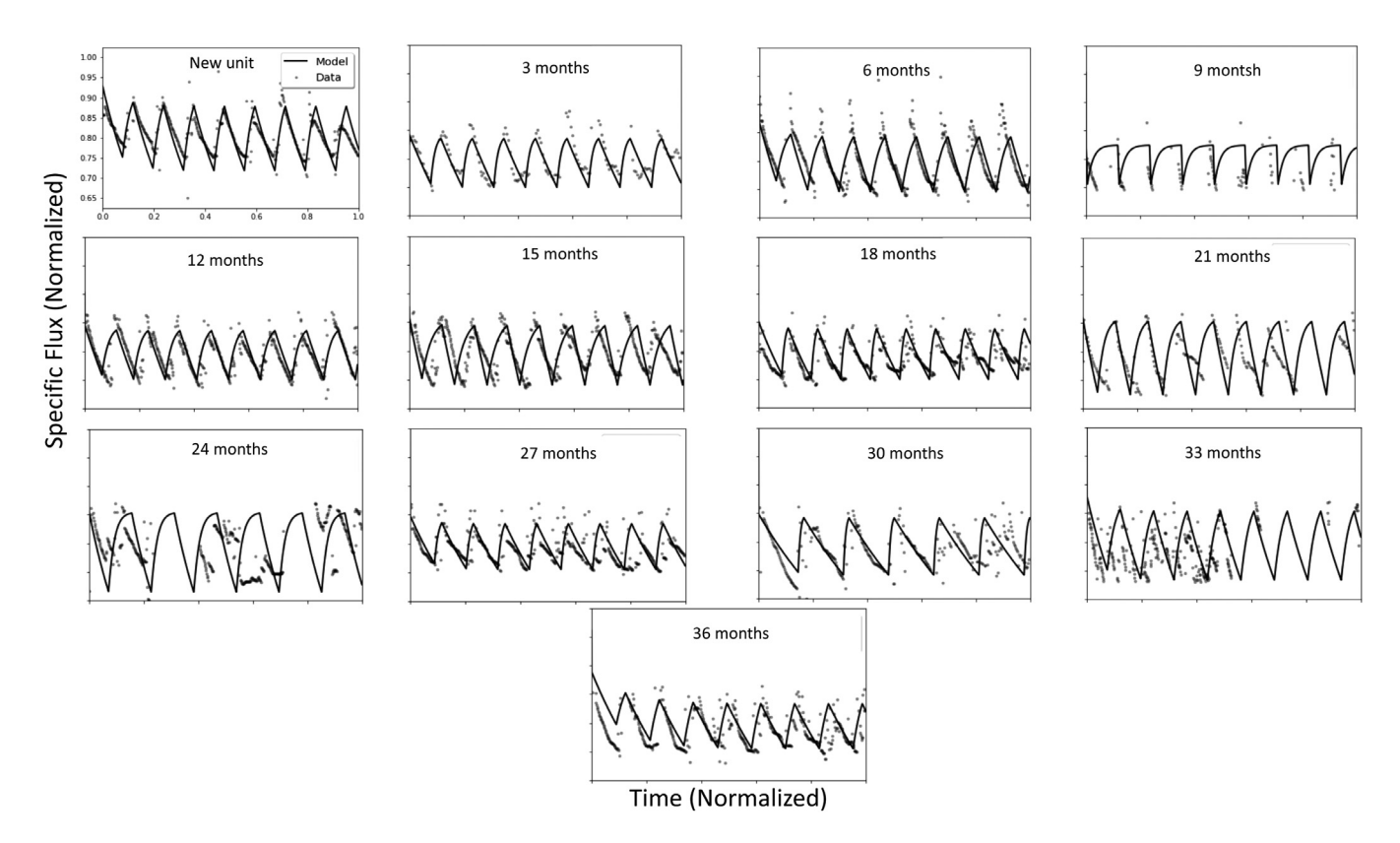


Fig. 1. Comparison between data and model for the best fit parameters. All figures share the same axis which has been normalized by the maximum observed specific flux. The newest unit is top left and units age left to right, top to bottom with the oldest unit in the bottom center. The relative errors are: 0.0098, 0.0089, 0.0115, 0.0118, 0.0122, 0.0054, 0.0099, 0.0054, 0.0050, 0.0035, 0.0031 and 0.0179, 0.0132. For each year (minimum, maximum and average specific flux) indicate the decline in production: (4.7, 7.4, 5.9), (5.0, 5.9, 5.1), (3.7, 5.4, 4.5), (4.0, 5.7, 4.3), (4.0, 5.7, 4.8), (4.0, 5.8, 4.9), (2.5, 5.5, 2.8), (3.5, 5.0, 3.8), (3.5, 5.4, 3.9), (2.5, 5.9, 3.2), (2.5, 5.9, 3.5), (2.5, 5.9, 3.2), (3.1, 5.1, 3.1).

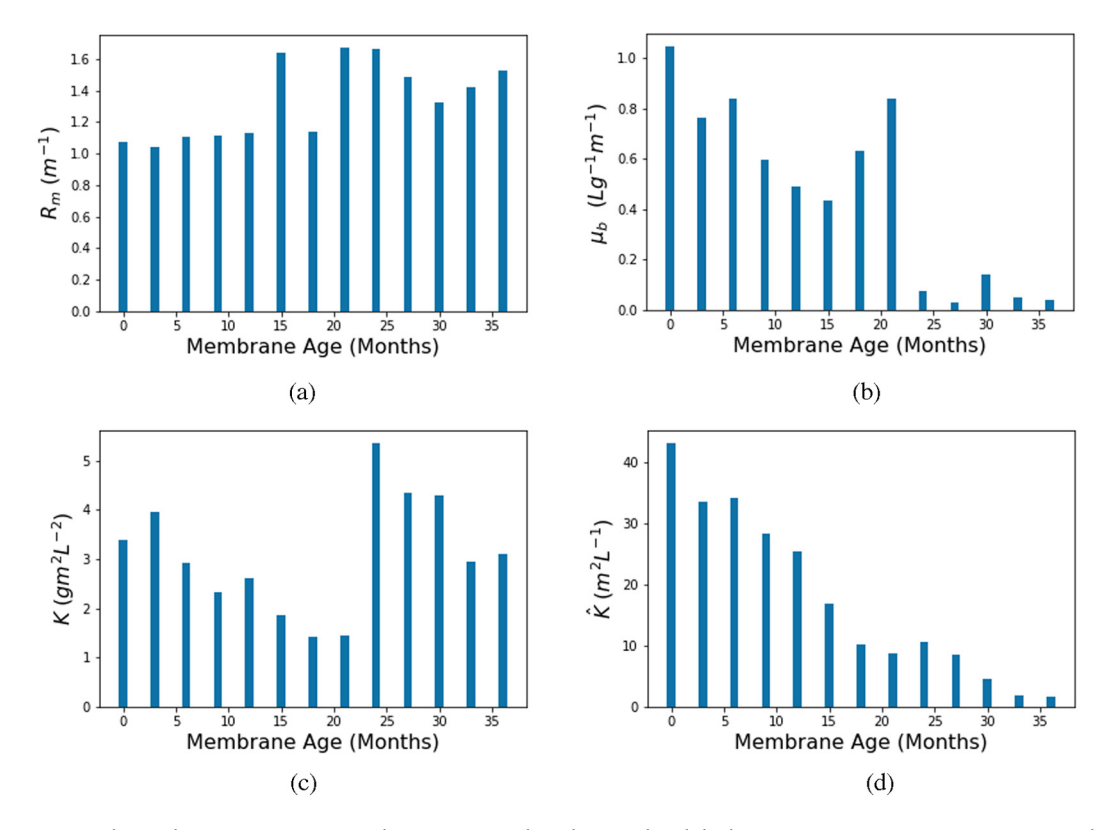


Fig. 2. Parameter estimates as the membrane unit ages. Fits were done 100 times with random initial seeds leading to some variation in parameter estimates shown using standard deviations as error bars. Notice that R_m increases about mid-way through the time period. There are dramatic changes in γ_b and K after months 21 and 24. The parameter governing the removal efficiency, \hat{K} , decays as the membrane ages.

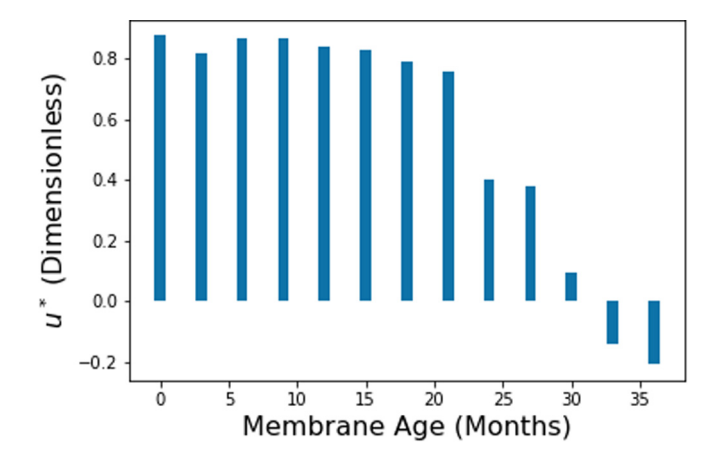


Fig. 3. This shows u^* as a function of membrane age. Initially it is more efficient to spend the majority of the time in forward operation. As the membrane ages, it requires more frequent reversals to maintain the optimal behavior. More frequent reversals eventually lead to more time in regeneration than filtration, hence u^* becomes negative.

intersects at a specific value of B, the dashed trajectories). Once the trajectory intersects the switching curve, a u^* that maintains the specific density of B associated with the crossing is determined.

Values of u^* between -1 and 1 have no physical meaning for the model since it implies both forward and reversal operation. This is handled by treating the optimal value of u^* to be the average of forward and backwards operation over the course of one cycle, defined to be a forward operation followed by a backwards operation. Thus, if $u^*=0$, an equal time is spent in forward and backwards operation. It is easy to translate u^* into a percentage of time spent in forwards operation: $\frac{1+u^*}{2} \times 100\%$. By increasing the frequency of cycling while keeping the average the same, approximating the optimal operation [26,28]. This method is consistent with the specific application where filtration alternates between forward and backwards operation in an essentially discontinuous manner on the time-scale of the observations.

The details of this implementation have been described previously for constant pressure operation and can be found in earlier studies [26,28]. In the Appendix, the method for constant flux operation is described, and the specific flux formulation is described in more detail.

It is straightforward to determine the optimal switching value. With an initially clean filter (B(0)=0), the filter is operated in forward filtration (e.g. u=1). Following the trajectory in the (B,λ) plane, the trajectory either hits the switching curve or does not. If not, there is no reason to reverse the flow — forward filtration is optimal. If the trajectory does hit the switching curve, the optimal strategy is to remain on that curve. This implies that B is at steady-state so Eq. (1) is used to determine the appropriate value of u^* :

$$u^* = \frac{B\hat{K} - K}{B\hat{K} + K}.$$

Notice that the specific geometry of the trajectories depend on the parameter values, hence the motivation for determining the parameter values in the previous sections.

Just as the parameters vary as the membrane ages, so does the optimal value of u^* . In Fig. 3, shows how u^* evolves as the membrane ages. For the first 21 months of operation, the model analysis suggests that $u^* \approx 0.8$ is optimal. This corresponds to approximately 93.5% of the time in forward operation. There is a rapid decline until at 36 months the prediction is that only 43% of the time should be spent in forward operation. This is consistent with the hypothesis that the aging of the membrane affects the operational behavior which is reflected in changing model parameter estimates. Therefore, the optimal timing and duration of backwashing is not a fixed estimate as is often currently practiced, but one that varies with the age of the membrane.

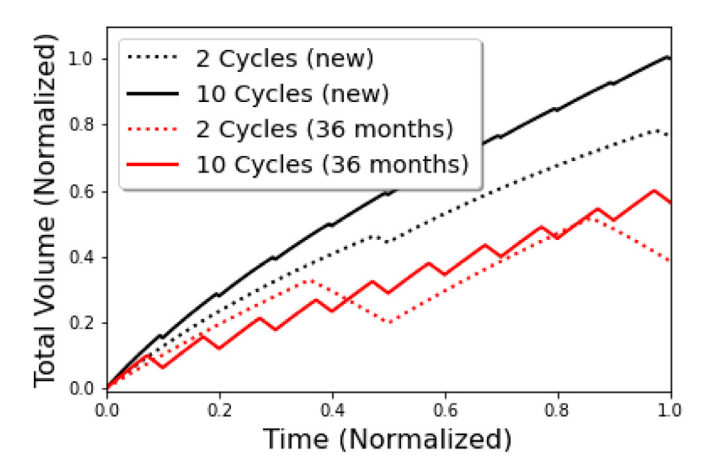


Fig. 4. Value of $\int_0^{T_{final}} J_{sp}(t)u(t)dt$ as a function of time (both normalized) for different filters and frequencies. The solid (dotted) lines are simulations for ten (two) full cycles. Black lines indicate parameters associated with new filters, while the red curves are those for units that have been in operation for 36 months. Note that higher frequency and newer filters provide more volume for the entire process.

Now consider the differences in both filter age as well as how to approximate the optimal solution using piecewise filtering, which is in-line with practical implementation where the flow direction is periodically reversed. During a filtration for T units of time, perform Nforward/backward cycles, where the percentage of time spent during a complete forward/backward cycle determined by u^* . Fig. 4 shows the value of $\int_0^{T_{final}} J_{sp}(t)u(t)dt$ as a function of time for either two or ten complete cycles and for both the newest and the oldest units — those that have been operated for 36 months. This is a measure of membrane performance since higher values relate to more water produced. Notice that as the number of cycles, N, increases so does the integral since it is getting closer to the theoretical optimal estimates. As expected, the more cycles that are used (e.g. the more times the flow is reversed), the higher the efficiency since this is closer to the theoretical optimal. However, even when using the optimal switching, the oldest units (36 months) are less efficient than the newer units, reflecting the effect of membrane age on the expected performance.

6. Conclusions

In previous studies [26,28], the focus was on constant pressure filtration where the optimization goal was to maximize the total filtered volume in a fixed period of time. In this manuscript, constant flux operation is considered, which is typical of real-world MF for environmental separations. In contrast with previous work, the forward and backward filtration problems are solved analytically and use these solutions for the optimal control problem. By parameterizing the model using data provided by OCWD, differences in key parameters for new and aged filtration units can be identified. Interestingly, even without considering the geometric aspects of the hollow fiber filters, reasonable estimates indicating clear differences in several key parameters with membrane age are obtained. The efficiency of regeneration declines as the filters age which is reflected in decreased \hat{K} . Analysis of the model indicates that hydraulic regeneration should be performed more often and for longer duration as the filter ages to more aggressively counter irreversible fouling. It is also shown that neglecting geometry does not appear to preclude the application of the model to other filtration methods. Thus this more tractable model can be used to probe interesting, operational aspects of membrane filtration. This does not argue that geometry can be neglected in every aspect of the problem, but this does provide strong motivation to continue developing models that do not require detailed geometric considerations. This demonstrates that irreversible fouling reduces microfiltration efficiency as is intuitively apparent. This analysis provides insight into how to counter the effects of membrane aging, while still aiming for optimal water production efficiency. It is emphasized that because data were collected from an operational full-scale facility, inherent variations in the feedwater characteristics would have also impacted productivity in addition to aging, which are impossible to separate in real-world situations. Specific hypotheses suitable for developing models for the evolution of specific parameters were not developed in this manuscript. Instead, the goal was interpreting the parameters obtained via parameterization and the understanding the subsequent effects of these parameter estimates on the predictions from the optimal control analysis. Other differences that may impact the model predictions for geometrically extended, spatial models include operational differences such as inside-out versus outside-in because the flow patterns may be substantially different. Those differences have not been addressed in the current study.

Note that there are multiple directions that will be explored in the near future. Primarily, assuming a linear relationship between the regeneration and the pressure may not address permanently irreversible attachment. Additionally, investigating the role of varying pressure drops during regeneration may provide more efficient foulant removal. Finally, it is necessary to investigate the scheduling of chemical and hydrodynamic removal in combination — which will allow for direct comparison to plant-scale data.

CRediT authorship contribution statement

N.G. Cogan: Conceptualization, Methodology, Formal analysis, Writing, Funding acquisition, Project management. Deniz Ozturk: Methodology, Formal analysis, Writing. Kenneth Ishida: Data curation, Review & editing. Jana Safarik: Data curation, Review & editing. Shankararaman Chellam: Conceptualization, Writing, Data curation, funding acquisition, Project management.

Declaration of competing interest

The authors declare that they have no known competing financial interests or personal relationships that could have appeared to influence the work reported in this paper.

Acknowledgments

N.C. was supported in part by NSF-CBET #1510743 S.C. was supported by NSF-CBET #1636104

Appendix

A.1. Nomenclature

See Table 2.

A.2. Differential equation analysis

During the forward filtration problem (e.g. while $u \equiv 1$), with an initially clean membrane the accumulation of foulant during the period $t = t_0$ to $t = t_1$ the solution of the foulant is given by,

$$B_{forward}(t) = KJt. (4)$$

Consider regeneration, where $u \equiv -1$ during the period between t_1 and t_2 is given by,

$$\frac{dB}{dt} = -\hat{K}JB$$

$$B(t_1) = KJt_1$$

The solution is,

$$B_{backwards}(t) = KJt_1 e^{-\hat{K}Jt}.$$
 (5)

 Table 2

 Description of variables and parameters used in this study.

Model variable	Description (units)
t	Time (h)
t_i	Time at the beginning/end of switching (h)
J_{sp}	Specific flux (L/(m ² h Pa))
ΔP	Pressure drop (Pa)
\boldsymbol{B}	Foulant density (g/L)
$B_{forward}$	Foulant density during forward operation (g/L)
$B_{backward}$	Foulant density during regeneration (g/L)
R_B	Foulant resistance (1/m)
и	Flow direction, control (dimensionless)
λ	Adjoint variable (g/L)
C	Constant of integration (g/L)
Ĉ	Constant of integration (g ² /L ²)
Parameter	Description (units)
J	Flux (L/(m ² h))
R_m	Membrane resistance (1/m)
γ_b	Fouling efficiency (L/(g m)))
K	Foulant accumulation (g m ² /L ²)
	Foulant removal (m ² /L)

One full cycle of accumulation and regeneration from t=0 to t_2 is then defined by

$$B(t) = \begin{cases} B_{forward}(t) & \text{if } 0 < t \le t_1 \\ B_{backwards}(t) & \text{if } t_1 < t \le t_2. \end{cases}$$

The solutions in the accumulation and regeneration times given in Eqs. (4) and (5) are used to build the solution for multiple cycles. The value of B at the end of the first regeneration cycle is used, when $t=t_2$ to find,

$$B(t_2) = KJt_1 e^{-\hat{K}J(t_2 - t_1)}$$

This provides the initial condition to generate the particular solution of the differential equation for second accumulation,

$$B_{forward}(t) = KJ(t-t_2) + KJt_1e^{-\hat{K}J(t_2-t_1)}$$

Then the amount of foulant that has accumulated on the membrane after the second accumulation phase, that ends at $t = t_3$, is the initial condition for the second regeneration phase, that is:

$$B_{backwards}(t_3) = KJ(t_3 - t_2) + KJt_1e^{-\hat{K}J(t_2 - t_1)}$$

Using this as the initial condition, the solution of the equation during the second regeneration phase is,

$$B_{backwards}(t) = \left(KJ(t_3 - t_2) + KJt_1 e^{-\hat{K}J(t_2 - t_1)}\right) e^{-\hat{K}J(t - t_3)}.$$

Clearly this can be generalized to an arbitrary number of cycles. In Fig. 5, examples of the dynamics of the membrane accumulation for eight cycles are shown. The two cases are distinguished by the ratio of the forward-to-backwards timing — panel (a) shows the accumulation/regeneration for longer time while panel (b) has a shorter regeneration cycle (i.e. more frequent backwashing). These figures show a few relevant behaviors. Note that for long backwashing, the foulant is completely removed — that is there is no irreversible fouling (left pane). However, if the backwashing is not sufficiently long, the membrane is never fully cleaned, even in the absence of irreversible attachment (right panel).

A.3. Optimal control analysis

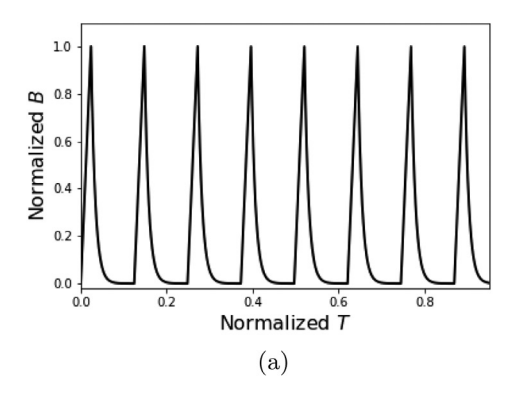
The optimal control problem is defined as,

$$\max_{u(t)} \int_0^{T_{final}} J_{sp}(t)u(t)dt = \max_{u(t)} \int_0^{T_{final}} \frac{u(t)}{R_m + \gamma_b B} dt \tag{6}$$

subject to the constraint,

$$\frac{dB}{dt} = \frac{(1+u)}{2}KJ - \frac{(1-u)}{2}\hat{K}JB,$$

$$R(0) = 0$$



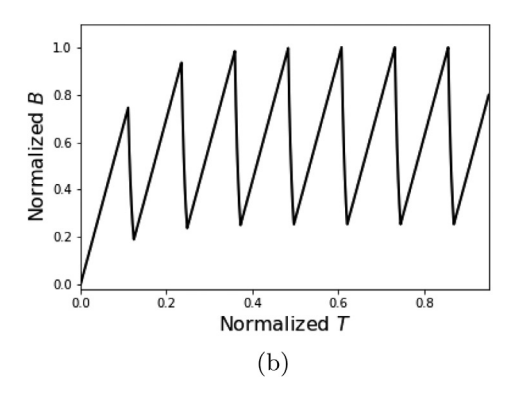


Fig. 5. Example of the dynamics of the accumulation and removal of the membrane foulant for eight cycles of forward/backwards operation. For demonstration purposes, the time and the total foulant accumulated are normalized. Note that *B* increases during forward operation, followed by a decrease during regeneration. The panel (a) shows the behavior when regeneration is performed for longer relative to forwards operation leading to clearance of the foulant. Panel (b) shows the behavior when the regeneration was relatively short. For short regeneration times the foulant is never fully removed even though an apparent periodic solution is obtained. This is not due to irreversible attachment, but merely the time-scale of fouling/regeneration.

Maximizing the specific flux, is directly related to maximizing the total volume of water that is filtered while minimizing the pressure used. By considering the previously filtered water used for backwashing, it is intuitively reasonable that maximizing the total water filtered must balance clearing the filter (regeneration that uses permeate water) and forward operation (that provides clean water, but causes the fouling). The goal here is to calculate this balance, and consider the effects of aging on the timing of backwashing.

Following Lenhart and Workman [44], the Hamiltonian functional is,

$$H(t, B(t), u(t), \lambda(t)) = \frac{u}{R_m + \gamma_b B} + \lambda \left(\frac{(1+u)}{2} KJ - \frac{(1-u)}{2} \hat{K}JB \right),$$
(7)
$$= \left(\frac{1}{R_m + \gamma_b B} + \frac{\lambda J}{2} (K + B\hat{K}) \right) u + \frac{\lambda J}{2} (K - \hat{K}B),$$
(8)
$$= \Omega u + \frac{\lambda J}{2} (K - \hat{K}B).$$
(9)

Where

$$\Omega = \left(\frac{1}{R_m + \gamma_h B} + \frac{\lambda J}{2} (K + B\hat{K})\right),\,$$

defines the curve in the state/adjoint domain that determines the separation between forward filtration and regeneration. Notice that the Hamiltonian is a linear function of control variable u. Pontryagin's principle tells us that maximizing the functional for the optimal control problem is identical to maximize the Hamiltonian. Therefore at $u = u^*$, the partial derivative of Hamiltonian with respect to the control variable u is equal to zero:

$$\Omega = \frac{\partial H}{\partial u} = \left(\frac{1}{R_m + \gamma_b B} + \frac{\lambda J}{2} (K + B\hat{K})\right) = 0$$

Since the Hamiltonian is linear in u this partial derivative does not yield any information about the control variable. Instead, the maximum and minimum values of the control function are examined and require that

 $H(u) \le H(u^*),$

if u^* is optimal. Therefore,

$$u^* = \begin{cases} 1 & \text{if } \Omega > 0 \\ -1 & \text{if } \Omega < 0 \\ unknown & \text{if } \Omega = 0 \end{cases}$$

Since
$$J \geq 0$$
,

$$\Omega > 0 \Rightarrow \lambda(K + B\hat{K}) > \frac{-2}{J(R_m + \gamma_b B)},$$

$$\Omega < 0 \Rightarrow \lambda(K + B\hat{K}) < \frac{-2}{J(R_m + \gamma_b B)},$$

$$\Omega = 0 \Rightarrow \lambda = \frac{-2}{J(K + B\hat{K})(R_m + \gamma_b B)}.$$

The curve $\lambda = \frac{-2}{J(K+B\hat{K})(R_m+\gamma_bB)}$ is the switching curve which determines the switching times between forwards and backwards for this optimal control problem. The geometry of the solution curves in (λ, B) plane provides the dynamics of the optimal filtration. The system of equations that define the state variable, B and adjoint variable λ need to be examined. These dynamics define the flux through Eq. (3)

$$\begin{split} \frac{dB}{dt} &= \frac{(1+u)}{2} KJ - \frac{(1-u)}{2} \hat{K}JB, \\ \frac{d\lambda}{dt} &= -\frac{\partial H}{\partial B} = \frac{\gamma_b u}{(R_m + \gamma_b B)^2} - \frac{\lambda J \hat{K}}{2} \end{split}$$

subject to the initial condition B(0) = 0 and the transversality condition $\lambda(0) = 0$

The trajectories during forward and backwards operation are solved separately. During forward operation, $u \equiv 1$, and,

$$\begin{split} \frac{dB}{dt} &= KJ \\ \frac{d\lambda}{dt} &= \frac{\gamma_b}{(R_m + \gamma_b B)^2}. \end{split}$$

By dividing these equations, a differential equation defined in the B/λ plane is found,

$$\frac{d\lambda}{dB} = \frac{\gamma_b}{KJ(R_m + \gamma_b B)^2}.$$

This has solution,

$$\lambda(B) = \frac{-1}{KJ(R_m + \gamma_h B)} + C. \tag{10}$$

The integration constant, C, is determined by applying initial conditions.

During the backward operation, $u \equiv -1$, and the equations become

$$\frac{dB}{dt} = -\hat{K}JB$$

$$\frac{d\lambda}{dt} = \frac{-\gamma_b}{(R_m + \gamma_b B)^2} - \frac{\lambda J\hat{K}}{2}.$$

Which can be written,

$$\frac{d\lambda}{dB} = \frac{\gamma_b}{\hat{K}JB(R_m + \gamma_b B)^2} + \frac{\lambda}{2B}$$

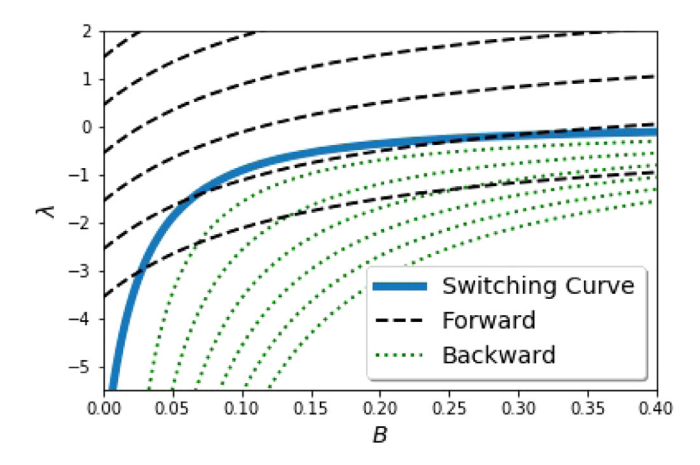


Fig. 6. Switching curve and trajectories in the B, λ plane.

The solution allows us to write the adjoint in terms of the foulant is,

$$\lambda(B) = \frac{-1}{\hat{K}JB(R_m + \gamma_b B)} + \frac{\hat{C}}{B}.$$

Where C and \hat{C} are integral constants for forward and backward curves and depend on the initial state. The switching curve and the forward filtration curves are hyperbolas, while the curves corresponding to the backward operation are logarithmic curves (see Fig. 6).

References

- Mesfin M. Mekonnen, Arjen Y. Hoekstra, Four billion people facing severe water scarcity. Sci. Adv. 2 (2) (2016) e1500323.
- [2] Elizabeth Hameeteman, Future Water (in)Security: Facts, Figures, and Predictions, Global Water Institute, 2013, pp. 1–16.
- [3] Alexandra S. Richey, Brian F. Thomas, Min-Hui Lo, John T. Reager, James S. Famiglietti, Katalyn Voss, Sean Swenson, Matthew Rodell, Quantifying renewable groundwater stress with GRACE, Water Resour. Res. 51 (7) (2015) 5217–5238.
- [4] L.S. Coplin, D. Galloway, Chapter 7: Houston–Galveston, Texas: Managing coastal subsidence, in: Devin L. Galloway, David Richard Jones, Steven E. Ingebritsen (Eds.), Land Subsidence in the United States, U.S. Department of the Interior and U.S. Geological Survey, US Geological Survey, Reston, VA, 1999, pp. 35–48.
- [5] S. Alspach, B. Adham, T. Cooke, P. Delphos, J. Garcia-Aleman, J. Jacangelo, A. Karimi, J. Pressman, J. Schaefer, S. Sethi, Microfiltration and Ultrafiltration Membranes for Drinking Water, Volume 100, (12) American Water Works Association, 2008.
- [6] M. Raffin, E. Germain, S.J. Judd. Influence of backwashing, Flux and temperature on microfiltration for wastewater reuse, Sep. Purif. Technol. 96 (2012) 147–153.
- [7] Hao Guo, Zihe Li, Jun Huang, Rongqing Zhou, Chongde Wu, Yao Jin, Microfiltration of soy sauce: Efficiency, resistance and fouling mechanism at different operating stages, Sep. Purif. Technol. 240 (2020) 116656.
- [8] Henry J. Tanudjaja, Jia Wei Chew, Critical flux and fouling mechanism in cross flow microfiltration of oil emulsion: Effect of viscosity and bidispersity, Sep. Purif. Technol. 212 (2019) 684-691.
- [9] Yuri A.R. Lebron, Victor R. Moreira, Tatiane P.B. Furtado, Selma C. da Silva, Lisete C. Lange, Miriam C.S. Amaral, Vinasse treatment using hybrid tannin-based coagulation-microfiltration-nanofiltration processes: Potential energy recovery, technical and economic feasibility assessment, Sep. Purif. Technol. 248 (2020) 117152.
- [10] Murielle Rabiller-Baudry, Patrick Loulergue, Jean Girard, Massoud El Mansour El Jastimi, Aurélie Bouzin, Marie Le Gallic, Alain Moreac, Philippe Rabiller, Consequences of membrane aging on real or misleading evaluation of membrane cleaning by flux measurements, Sep. Purif. Technol. (2020) 118044.
- [11] Nicandro Porcelli, Simon Judd, Chemical cleaning of potable water membranes: A review, Sep. Purif. Technol. 71 (2) (2010) 137–143.
- [12] Henrik S. Marke, Martin P. Breil, Ernst Broberg Hansen, Manuel Pinelo, Ulrich Krühne, Investigation of the velocity factor in a rotational dynamic microfiltration system, Sep. Purif. Technol. 220 (2019) 69–77.
- [13] Ryo Makabe, Kazuki Akamatsu, Shin-ichi Nakao, Mitigation of particle deposition onto membrane surface in cross-flow microfiltration under high flow rate, Sep. Purif. Technol. 160 (2016) 98–105.
- [14] Shankararaman Chellam, Mark R. Wiesner, Evaluation of crossflow filtration models based on shear-induced diffusion and particle adhesion: complications induced by feed suspension polydispersivity, J. Membr. Sci. 138 (1) (1998) 83-97

- [15] Wei-Ming Lu, Shang-Chung Ju, Selective particle deposition in crossflow filtration, Sep. Sci. Technol. 24 (7–8) (1989) 517–540.
- [16] Haiqing Chang, Heng Liang, Fangshu Qu, Baicang Liu, Huarong Yu, Xing Du, Guibai Li, Shane A. Snyder, Hydraulic backwashing for low-pressure membranes in drinking water treatment: A review, J. Membr. Sci. 540 (2017) 362–380.
- [17] Xianhui Li, Yinghiu Mo, Jianxin Li, Wenshan Guo, Huu Hao Ngo, In-situ monitoring techniques for membrane fouling and local filtration characteristics in hollow fiber membrane processes: A critical review, J. Membr. Sci. 528 (2017) 187–200.
- [18] Ebrahim Akhondi, Farhad Zamani, Keng Han Tng, Gregory Leslie, William B. Krantz, Anthony G. Fane, Jia Wei Chew, The performance and fouling control of submerged hollow fiber (HF) systems: a review, Appl. Sci. 7 (8) (2017) 765.
- [19] Ebrahim Akhondi, Filicia Wicaksana, Anthony Gordon Fane, Evaluation of fouling deposition, fouling reversibility and energy consumption of submerged hollow fiber membrane systems with periodic backwash, J. Membr. Sci. 452 (2014) 319–331.
- [20] Yun Ye, Vicki Chen, Pierre Le-Clech, Evolution of fouling deposition and removal on hollow fibre membrane during filtration with periodical backwash, Desalination 283 (2011) 198–205.
- [21] Shankararaman Chellam, Joseph G. Jacangelo, Existence of critical recovery and impacts of operational mode on potable water microfiltration, J. Environ. Eng. 124 (12) (1998) 1211–1219.
- [22] Georges Belfort, Membrane modules: comparison of different configurations using fluid mechanics, J. Membr. Sci. 35 (3) (1988) 245–270.
- [23] Shankararaman Chellam, Mei Liu, Effect of slip on existence, uniqueness, and behavior of similarity solutions for steady incompressible laminar flow in porous tubes and channels, Phys. Fluids 18 (8) (2006) 083601.
- [24] Ruiyu Wu, Kuizu Su, Zhidong Wang, Tianwei Hao, Shaogen Liu, A comprehensive investigation of filtration performance in submerged hollow fibre membrane modules with different fibre geometries, Sep. Purif. Technol. 221 (2019) 93–100.
- [25] Frank Vinther, Ann-Sofi Jönsson, Modelling of optimal back-shock frequency in hollow-fibre ultrafiltration membranes II: Semi-analytical mathematical model, J. Membr. Sci. 506 (2016) 137–143.
- [26] N.G. Cogan, Shankararaman Chellam, A method for determining the optimal back-washing frequency and duration for dead-end microfiltration, J. Membr. Sci. 469 (2014) 410–417.
- [27] Nesrine Kalboussi, Jérôme Harmand, Alain Rapaport, Térence Bayen, Fatma Ellouze, Nihel Ben Amar, Optimal control of physical backwash strategy-towards the enhancement of membrane filtration process performance, J. Membr. Sci. 545 (2018) 38–48.
- [28] N.G. Cogan, Jian Li, Appala Raju Badireddy, Shankararaman Chellam, Optimal backwashing in dead-end bacterial microfiltration with irreversible attachment mediated by extracellular polymeric substances production, J. Membr. Sci. 520 (2016) 337–344.
- [29] Shona Robinson, Pierre R. Bérubé, Membrane ageing in full-scale water treatment plants. Water Res. 169 (2020) 115212.
- [30] Shona J. Robinson, Pierre R. Bérubé, Seeking realistic membrane ageing at bench-scale, J. Membr. Sci. 618 (2021) 118606.
- [31] Vera Puspitasari, Anthony Granville, Pierre Le-Clech, Vicki Chen, Cleaning and ageing effect of sodium hypochlorite on polyvinylidene fluoride (PVDF) membrane, Sep. Purif. Technol. 72 (3) (2010) 301–308.
- [32] Shima Hajibabania, Alice Antony, Greg Leslie, Pierre Le-Clech, Relative impact of fouling and cleaning on PVDF membrane hydraulic performances, Sep. Purif. Technol. 90 (2012) 204–212.
- [33] Shona Robinson, Syed Zaki Abdullah, Pierre Bérubé, Pierre Le-Clech, Ageing of membranes for water treatment: Linking changes to performance, J. Membr. Sci. 503 (2016) 177–187.
- [34] C. Regula, Emilie Carretier, Yvan Wyart, Geneviève Gésan-Guiziou, A. Vincent, D. Boudot, Philippe Moulin, Chemical cleaning/disinfection and ageing of organic uf membranes: A review, Water Res. 56 (2014) 325–365.
- [35] Shankararaman Chellam, N.G. Cogan, Colloidal and bacterial fouling during constant flux microfiltration: Comparison of classical blocking laws with a unified model combining pore blocking and eps secretion, J. Membr. Sci. 382 (1–2) (2011) 148–157.
- [36] N.G. Cogan, M.Y. Hussaini, Shankararaman Chellam, Uncertainty propagation in a model of dead-end bacterial microfiltration using fuzzy interval analysis, J. Membr. Sci. 546 (2018) 215–224.
- [37] GWRS Operation Optimization Plan, DDB Engineering, Inc., Laguna Niguel, CA, 2015
- [38] Syed Z. Abdullah, Pierre R. Bérubé, Filtration and cleaning performances of PVDF membranes aged with exposure to sodium hypochlorite, Sep. Purif. Technol. 195 (2018) 253–259.
- [39] K.H. Tng, A. Antony, Y. Wang, G.L. Leslie, Membrane ageing during water treatment: mechanisms, monitoring, and control, in: A. Basile, A. Cassano, N.K. Rastogi (Eds.), Advances in Membrane Technologies for Water Treatment, Chapter 11: Membrane Ageing During Water Treatment: Mechanisms, Monitoring, and Control, Elsevier, 2015, pp. 349–378.

- [40] A. Antony, G. Leslie, Degradation of polymeric membranes in water and wastewater treatment, in: A. Basile, A. Cassano S. Nunes (Eds.), Advanced Membrane Science and Technology for Sustainable Energy and Environmental Applications, Chapter 22: Degradation of Polymeric Membranes in Water and Wastewater Treatment, Elsevier, 2011, pp. 718–745.
- [41] Rainer Storn, Kenneth Price, Differential evolution—a simple and efficient heuristic for global optimization over continuous spaces, J. Global Optim. 11 (4) (1997)
- [42] OCWD: https://www.ocwd.com/gwrs/frequently-asked-questions/, 2021.
- [43] A. Touffet, J. Baron, B. Welte, M. Joyeux, B. Teychene, H. Gallard, Impact of pretreatment conditions and chemical ageing on ultrafiltration membrane performances. diagnostic of a coagulation/adsorption/filtration process, J. Membr. Sci. 489 (2015) 284–291.
- [44] Suzanne Lenhart, John T. Workman, Optimal Control Applied To Biological Models, Chapman and Hall/CRC, 2007.
- [45] Lorenz T. Biegler, Ignacio E. Grossmann, Retrospective on optimization, Comput. Chem. Eng. 28 (8) (2004) 1169–1192.
- [46] N.G. Cogan, Shankar Chellam, Incorporating pore blocking, cake filtration, and eps production in a model for constant pressure bacterial fouling during dead-end microfiltration, J. Membr. Sci. 345 (1–2) (2009) 81–89.
- [47] N.G. Cogan, Shankararaman Chellam, Global parametric sensitivity analysis of a model for dead-end microfiltration of bacterial suspensions, J. Membr. Sci. 537 (2017) 119–127.